# Real-Time Kinetics of Ligand/Cell Surface Receptor Interactions in Living Cells: Binding of Epidermal Growth Factor to the Epidermal Growth Factor Receptor†

John C. Wilkinson,‡ Richard A. Stein,‡ Cheryl A. Guyer,‡ Joseph M. Beechem,§,|| and James V. Staros*,‡

*Department of Biological Sciences and Department of Molecular Physiology and Biophysics, Vanderbilt University, Nashville, Tennessee 37235*

*Received April 6, 2001; Revised Manuscript Received June 22, 2001*

ABSTRACT: We describe a system for extending stopped-flow analysis to the kinetics of ligand capture and release by cell surface receptors in living cells. While most mammalian cell lines cannot survive the shear forces associated with turbulent stopped-flow mixing, we determined that a murine hematopoietic precursor cell line, 32D, is capable of surviving rapid mixing using flow rates as great as 4.0 mL/s, allowing rapid processes to be quantitated with dead times as short as 10 ms. 32D cells do not express any endogenous epidermal growth factor (EGF) receptor or other ErbB family members and were used to establish monoclonal cell lines stably expressing the EGF receptor. Association of fluorescein-labeled H22Y-murine EGF (F-EGF) to receptor-expressing 32D cells was observed by measuring time-dependent changes in fluorescence anisotropy following rapid mixing. Dissociation of F-EGF from EGF-receptor-expressing 32D cells was measured both by chase experiments using unlabeled mEGF and by experiments in which equilibrium was perturbed by dilution. Comparison of these dissociation experiments showed that little, if any, ligand-induced dissociation occurs in the chase dissociation experiments. Data from a series of association and dissociation experiments, performed at various concentrations of F-EGF in the nanomolar range and at multiple cell densities, were simultaneously analyzed using global analysis techniques and fit to a two independent receptor-class model. Our analysis is consistent with the presence of two distinct receptor populations having association rate constants of $k_{on1} = 8.6 \times 10^6\ M^{-1}\ s^{-1}$ and $k_{on2} = 2.4 \times 10^6\ M^{-1}\ s^{-1}$ and dissociation rate constants of $k_{off1} = 0.17 \times 10^{-2}\ s^{-1}$ and $k_{off2} = 0.21 \times 10^{-2}\ s^{-1}$. The magnitudes of these parameters suggest that under physiological conditions, in which cells are transiently exposed to nanomolar concentrations of ligand, ligand capture and release may function as the first line of regulation of the EGF receptor-induced signal transduction cascade.

Epidermal growth factor (EGF)[1] is a 53 amino acid polypeptide hormone (*3*) that binds to and activates the EGF receptor on the plasma membrane of target cells (*4*). EGF was the first protein discovered in a family of structurally related growth factors including transforming growth factor α (TGFα) (*5*), amphiregulin (*6*), epiregulin (*7*), betacellulin (*8*), heparin-binding EGF-like growth factor (HB-EGF) (*9*), and heregulins 1−4 (*10*−*13*). These ligands can be further subdivided on the basis of the receptor types they activate (*14*). The EGF receptor (ErbB1) (*15*) is the prototype of the type I receptor tyrosine kinase family and is one of four evolutionarily related ErbB receptors (*16*), including ErbB2 (*17*), ErbB3 (*18*, *19*), and ErbB4 (*20*), that are activated by EGF-like ligands. Upon ligand binding these receptors dimerize to form either homodimers or heterodimers, which can vary in composition depending upon the activating ligand and the pattern of receptor expression (*21*). Dimerization activates the intracellular protein tyrosine kinase domain of the receptors (*22*) (with the exception of the kinase-impaired ErbB3 receptor), and signal propagation occurs either by phosphorylation of residues within the receptor tail that serve as docking sites for adaptor proteins containing Src-homology 2 (SH2) or phosphotyrosine binding (PTB) domains or by direct phosphorylation of substrates. Depending on the composition of the ErbB dimer pair, different subsets of adaptor proteins may be recruited and different substrates may be phosphorylated, thereby providing signal diversification through the EGF-like ligand/ErbB receptor network (*23*). A common theme among cellular responses to ErbB dimer

† This work was supported by Grants R01 GM55056 and T32 GM08320 from the National Institutes of Health. Preliminary accounts of this work were presented at the 1999 Protein Society annual meeting (*1*) and the 2000 Biophysical Society annual meeting (*2*).

* Corresponding author address: Department of Biological Sciences, Vanderbilt University, VU Station B 351634, Nashville, TN 37235-1634. Telephone: (615)-343-4341. Fax: (615)-343-6707. E-mail: james.v.staros@vanderbilt.edu.

‡ Department of Biological Sciences.

§ Department of Molecular Physiology and Biophysics.

|| Present address: Molecular Probes, Inc., 4849 Pitchford Avenue, Eugene, OR 97402.

[1] Abbreviations: AcCN, acetonitrile; BSA, bovine serum albumin; CMF−PBS, $Ca^{2+}$, $Mg^{2+}$-free phosphate-buffered saline; EGF, epidermal growth factor; mEGF, murine EGF; rEGF, rat EGF; FACS, fluorescence-activated cell-sorting; FBS, fetal bovine serum; FITC, fluorescein 5-isothiocyanate; FITC-EGF, fluorescein-labeled wild-type mEGF; F-EGF, fluorescein-labeled H22Y-mEGF; MAPK, mitogen-activated protein kinase; PTB, phosphotyrosine-binding; PI, propidium iodide; RP-HPLC, reverse-phase high-performance liquid chromatography; SDS, sodium dodecyl sulfate; SFB, stopped-flow buffer; SH2, src-homology 2; SPR, surface plasmon resonance; TGFα, transforming growth factor α; TEA, triethylamine; TFA, trifluoroacetic acid; WCM, WEH1-3B conditioned medium.

10.1021/bi010705t CCC: $20.00 
Published on Web 07/31/2001

activation is stimulation of DNA synthesis leading to cell division.

The binding of ligand to receptor is the primary event in initiation of signal transduction through the ErbB receptor family, and many studies have been performed to characterize this process. Of the possible ligand/receptor binding interactions, the binding of EGF to the EGF receptor is the most thoroughly characterized. Thermodynamically, this has often been measured in vitro by equilibrium binding of a radioactive ligand to cultured cells that express more than one ErbB receptor. After the amount of ligand bound is determined, the data are frequently analyzed using a Scatchard transformation (*24*), which in the case of EGF binding to the EGF receptor often yields a curvilinear plot interpreted to indicate the presence of two independent receptor populations (*22*, *25*, *26*). This approach has drawbacks that include the potential for ErbB heterodimerization, the uncharacterized nature of radioactively labeled hormone, and the inherent, and often erroneous, assumptions associated with using Scatchard analysis (*27*), particularly those regarding ligand depletion. More recently, our laboratory has reported a method for examining the thermodynamics of interaction between EGF and the EGF receptor by flow cytometry in which the effects of ligand depletion were taken into account (*28*). In this study, binding was observed of a fluorescent derivative of EGF to cells that express the EGF receptor in the absence of other ErbB proteins. By using a well-characterized, homogeneous ligand and measuring binding at several cell densities, many of the technical problems associated with previous binding studies were overcome, leading to a more accurate description of EGF/EGF receptor equilibrium binding properties.

While these equilibrium studies have been useful for testing potential binding mechanisms as well as determining ligand/receptor affinities, they provide no information about the kinetics of binding between ligand and receptor. Recent evidence suggests that these kinetic processes may have a role in determining the physiological response of cells to ligand (*29*). Therefore, a detailed study of the kinetic parameters governing ligand/receptor interactions in intact cells is warranted.

Many groups have performed pre-steady-state experiments using $^{125}$I-EGF and intact cells in order to determine kinetic rate constants (*30*−*33*). In these experiments $^{125}$I-EGF is incubated with cells for defined amounts of time prior to extensive washing and determination of the amount of radioligand bound. By examination of the amount of ligand bound over time in this manner, rate constants were determined. However these experiments suffer from disadvantages similar to those for equilibrium studies using radioactive ligands, as well as low data sampling rates over the binding period and small data sets. Possibly owing to these complications, a variety of association and dissociation rate constants have been reported, and differences exist concerning the number of rate constants required to describe the data.

In addition to radioligand binding to intact cells, several kinetic studies examining EGF binding to the extracellular domain of the EGF receptor (EGFR-ED) have been reported. These experiments have been performed in vitro through the use of surface plasmon resonance (SPR) measurements (*29*, *34*, *35*). In these experiments, one component (generally EGF) is immobilized onto the dextran layer of a sensor chip in a microflow cell while a solution containing the second component (generally EGFR-ED) is flowed over the immobilized ligand. Through the use of this technique, kinetic measurements can be made in real-time, and high sampling rates over the binding period may be achieved. However, comparison of SPR measurements to those using intact cells shows that rate constants and calculated $K_d$ values vary by as much as 3 orders of magnitude between the two methods. These differences may reflect technical problems associated with SPR experiments (*36*) or intrinsic differences between binding kinetics of soluble EGFR-ED and full length EGF receptor at the surface of a cell.

The application of fluorescence spectroscopy to the study of EGF/EGF receptor interactions has overcome several of the limitations imposed by the above methods. Unlike $^{125}$I-EGF binding experiments, fluorescence spectroscopy allows the heterogeneity of the ligand to be reduced, and high sampling rates over the binding period may be achieved. Fluorescence spectroscopy offers an improvement over SPR measurements in that experiments may be performed using intact cells. In one study, Carraway and Cerione applied fluorescence spectroscopy to examine the kinetic interaction of a fluorescent derivative of EGF with suspended A431 cells (*37*). They showed that fluorescence provided a sensitive measure of association and dissociation of EGF with the EGF receptor; however, no detailed analysis of the observed kinetic interactions was undertaken. In a more recent study, Gross and co-workers used fluorescence microscopy to observe the interaction of EGF with single A431 cells (*38*). However a large number of data sets were not obtained for use in kinetic analysis, possibly due to limitations of performing experiments on single cells. While both of these studies obtained high sampling rates over the binding periods, improving the precision of kinetic measurements, each study employed cells that are heterogeneous for ErbB receptor expression. To date, no detailed kinetic study of which we are aware has been reported in which the binding of EGF to intact cells expressing the EGF receptor in the absence of other ErbB proteins was observed.

Previous work in our laboratory utilized stopped-flow fluorescence spectroscopy to study the kinetics of EGF/EGF receptor interactions in a cell membrane preparation (*39*). Using A431 membrane vesicles as a source of EGF receptor, the binding of fluorescein-labeled wild-type mEGF (FITC-EGF) was observed in real-time by measuring changes in ligand anisotropy. Free EGF has a low anisotropy, and receptor-bound EGF has a high anisotropy. By the monitoring of changes in ligand anisotropy over time following stopped-flow mixing, performed over a wide range of FITC-EGF concentrations and several dilutions of membranes, a very precise and highly sensitive determination of the association and dissociation rates governing this interaction was obtained.

Here we report the extension of stopped-flow fluorescence anisotropy measurements for measuring the binding of EGF to its receptor in living cells. By using cells that are capable of surviving the stopped-flow mixing process and that are engineered to express the EGF receptor in the absence of other ErbB proteins, we have measured the binding of fluorescein-labeled H22Y-murine EGF (F-EGF) to living cells in real-time. Global analysis of real-time data is

consistent with a two independent receptor-class model. The magnitudes of the kinetic parameters obtained suggest that under physiological conditions, in which cells are transiently exposed to nanomolar concentrations of ligand, ligand capture and release may function as the first line of regulation of the EGF receptor-mediated signal transduction cascade.

## MATERIALS AND METHODS

*Materials.* Murine EGF (mEGF) was prepared as previously described (*40*). HPLC solvents were from Burdick and Jackson. Trifluoroacetic acid (TFA) (HPLC grade) and triethylamine (TEA) (Sequanal grade) were from Pierce. Fluorescein 5-isothiocyanate (FITC) was from Molecular Probes (F-1906). All aqueous solutions were prepared using water purified with a Mill-Q water system (Millipore). Propidium iodide (PI) and bovine serum albumin (BSA), as well as all buffers and salts, were from Sigma. Fetal bovine serum (FBS) and RPMI-1640 were from Gibco. G418 sulfate was from Mediatech. Sodium dodecyl sulfate (SDS) was from Serva. All other chemicals were ACS reagent grade or better.

*Preparation of Fluorescein-Labeled H22Y-mEGF (F-EGF).* The expression and purification of H22Y-mEGF has been described (*28*). The affinity of H22Y-mEGF, as measured by competition binding assays against wild-type mEGF, and biological activity, as measured by stimulation of autophosphorylation, were determined as previously described (*39*). Labeling and purification of H22Y-mEGF with fluorescein isothiocyanate was carried out as previously described for wild-type mEGF (*39*). Purity of the final labeled product was verified by reverse-phase HPLC (RP-HPLC) using a 4.6 × 220 mm Brownlee Aquapore RP-300 column with 0.1% TFA in water (buffer A) and 0.1% TFA in 20:80 water/AcCN (buffer B) as mobile phases. The solvent delivery system consisted of two Waters 515 pumps, and the absorbance at 220, 280, and 440 nm was monitored with a Waters 996 photodiode array detector, with the system controlled from a Millennium 32 workstation. Prior to the HPLC run, the column was equilibrated with 95:5 buffer A/buffer B and the product was eluted with a 70 min linear gradient of 5−50% buffer B at a flow rate of 1 mL/min. The concentration of purified F-EGF was calculated from the absorbance using $\epsilon_{280} = 36\,000\ cm^{-1}\,M^{-1}$ (*39*). To verify the mass of the final product, matrix-assisted laser desorption ionization time-of-flight (MALDI-TOF) mass spectrometry was performed using a PerSeptive Biosystems Voyager-DE STR mass spectrometer and a matrix of sinapinic acid (3,5-dimethoxy-4-hydroxycinnamic acid).

*Cell Culture.* The IL-3 dependent hematopoietic progenitor cell line 32D (gift of G. Carpenter, Vanderbilt University) was maintained in RPMI-1640 containing 15% fetal bovine serum (FBS) and 5% WEH1-3B conditioned medium (WCM) as a source of IL-3. WT3 cells (an EGF receptor-expressing 32D subline (*28*)) and LE1.15 cells (described below) were maintained in RPMI-1640/15% FBS/5% WCM + 750 $\mu$g/mL G418. Cells were grown at 37 °C in an atmosphere of 5% $CO_2$/95% air.

*Cell Harvesting, Washing, and Density Determination.* Cells were harvested by centrifugation at 2500*g* for 5 min. Following removal of residual medium, cells were washed by resuspending cell pellets in 5−50 mL of $Ca^{2+}$, $Mg^{2+}$-free phosphate-buffered saline (CMF−PBS; 137.0 mM NaCl, 8.0 mM $Na_2HPO_4$, 2.7 mM KCl, 1.5 mM $KH_2PO_4$). Cell density was determined either by counting using a Coulter Z1 particle counter or by spectrophotometry, where $Abs_{600nm} = 0.5$ corresponds to $1.8 \times 10^6$ cells/mL, as determined by calibration with Coulter counting. This absorbance-to-density ratio was linear for absorbance values up to 1.0, and cell suspensions that exceeded this value were diluted prior to determination of density.

*Establishment of EGFR-Expressing 32D Cells.* 32D cells were harvested, residual medium was removed, and cells were resuspended in CMF−PBS at a density of $3 \times 10^7$ cells/mL. Cell suspension (300 $\mu$L) was placed in a 0.4 cm BioRad electroporator cuvette and mixed with 10 $\mu$g of the expression vector pLTR2-EGFR-neo (gift of P. P. Di Fiore, European Institute of Oncology). Electroporation was carried out using a BioRad GenePulser II electroporator set at 950 $\mu$F and 300 V. Following transfection, cells were immediately suspended in 10 mL of RPMI-1640/15% FBS/5% WCM and allowed to recover for 18 h prior to selection by the addition of 750 $\mu$g/mL G418. Clonal cell lines were established by fluorescence-activated cell-sorting (FACS) as follows: Transfected cells arising from selection were harvested and washed once with CMF−PBS. Cells were equilibrated with F-EGF by resuspension at a density of $0.5 \times 10^6$ cells/mL in CMF−PBS + 0.1% BSA containing 20 nM F-EGF for 20 min at 4 °C. Cells were then analyzed for EGF receptor expression using a Becton-Dickinson FACStar-plus flow cytometer equipped with a Clone-Cyt integrated deposition system and Cellquest software. Once EGF receptor expression was confirmed, cloning was carried out by sorting single cells of the desired fluorescence, and thus EGF receptor expression, into wells of a 96-well microtiter plate containing RPMI-1640/15% FBS/5% WCM. Once putative clonal cell populations grew to sufficient density, cells were reanalyzed as described above to determine relative EGF receptor expression and monoclonality. Through this procedure several monoclonal 32D sublines expressing the EGF receptor were established. One clonal cell line in particular, named LE1.15, was used for subsequent kinetic experiments on the basis of its high level of EGF receptor expression.

*Cell Viability following Mixing.* 32D cells were harvested, washed twice with CMF−PBS, and resuspended in stopped-flow buffer (SFB: CMF−PBS + 0.1% BSA) at a density of $12.5 \times 10^6$ cells/mL. Cells were loaded into an SFM-4 mixing unit (described below), and 100 $\mu$L of cell suspension was mixed with 100 $\mu$L of SFB at various flow rates (0.67, 1.0, 2.0, and 4.0 mL/s). Five replicate mixes at each flow rate were performed. Following mixing at each flow rate, cells were collected and stained with propidium iodide (2 $\mu$g/mL final concentration) prior to assessing cell viability using a Becton-Dickinson FACScaliber flow cytometer. Controls consisted of unmixed cells or cells heat shocked for 30 min at 50 °C. Additional mixing experiments at the 0.67 mL/s flow rate were performed as above using the EGF receptor-expressing 32D subline LE1.15.

*EGF Receptor Internalization.* Internalization was measured by adaptation of previously described methods (*41*). Briefly, exponentially growing LE1.15 cells were harvested and resuspended in serum-free RPMI-1640. Following incubation at 37 °C for 3 h, cells were harvested and resuspended in cold binding buffer (RPMI-1640 + 0.1%

BSA) containing $^{125}$I-rEGF (10 ng/mL, specific activity 2 $\times$ $10^4$ cpm/ng) (gift of W. Russell, Vanderbilt University). Background samples were prepared in which the binding buffer was supplemented with a 100-fold excess of unlabeled mEGF. Following incubation on ice for 90 min, aliquots (0.5 mL) were removed and placed in 1.5 mL eppendorf tubes at either 37 or 20 °C for various amounts of time from 0 to 90 min. Following incubation at the appropriate temperatures, all tubes were placed on ice. To separate cell-associated radioactivity from free radioactivity, samples were centrifuged at 2500*g* for 4 min through a cushion of serum (0.7 mL). The cell pellets were then washed twice in cold acid strip buffer (150 mM acetic acid, 150 mM NaCl, pH 2.7) to remove cell surface radioactivity. The acid washes were saved, and the final cell pellet was solublized using 100 mM NaOH + 0.1% SDS. Radioactivity in both the acid washes and the solublized cell samples was determined using a Beckman Gamma 4000 counter.

*Real-Time Association of F-EGF to LE1.15 Cells.* All stopped-flow mixing experiments were performed with an SFM-4 stopped-flow unit (Molecular Kinetics) equipped with an FC.15 fluorescence cuvette (35 $\mu$L of working volume) and a hard-stop shutter. All mixing was performed using a 0.667 mL/s flow rate resulting in an instrument dead time of approximately 50 ms. Fluorescence detection was accomplished by attaching a homemade emission channel mounting platform on each side of the SFM-4 mixing unit such that two emission channels could be mounted in T-format geometry and aligned with the cuvette. Each detection channel consisted of a collimating lens (Oriel), a Glan-Thompson polarizer, and a narrow band-pass filter centered at 520 nm (Oriel). An R-928 photomultiplier tube (PMT) (Hammamatsu) was mounted on the end of each emission channel. Signals from each PMT were amplified using an SR445 DC-300 amplifier (Stanford Research), and discriminated using a SR400 two-channel photon counter (Stanford Research). Discriminator output for each channel was detected using an MCS-II multichannel scalar board (Canberra) mounted in an Intel 486DX-based microcomputer. Data acquisition by the MCS-II boards (8192 channels total) was synchronized with the stopped-flow unit by the external synchronization output of the SFM-4 controller unit. The excitation light source was an Innova model 310 argon ion laser (Coherent) tuned to 488 nm and operated at constant power. The beam was attenuated as necessary to maintain counting levels below 300 000 counts/s, minimizing photobleaching and remaining within the linear counting range of the detection electronics.

Exponentially growing LE1.15 cells were harvested, washed twice with CMF−PBS, and resuspended in SFB at 3.2 $\times$ $10^6$, 5.8 $\times$ $10^6$, and 12.2 $\times$ $10^6$ cells/mL prior to storage on ice. Aliquots of cells were allowed to equilibrate to 20 °C before loading into the SFM-4 syringes. The temperature of all syringes was maintained at 20 °C by a circulating water bath. For F-EGF binding experiments, 100 $\mu$L of cells at each density was mixed with 100 $\mu$L of F-EGF stocks to give final cell densities of 1.6 $\times$ $10^6$, 2.9 $\times$ $10^6$, or 6.1 $\times$ $10^6$ cells/mL and final F-EGF concentrations of 1.0, 1.5, 2.0, 3.0, 5.0, 7.5, 10, and 15 nM. Data were acquired at 38 ms intervals starting 10 s before mixing, and time zero was determined as the first data point taken after the stepper motors of the stopped-flow unit stopped. This resulted in a total of 7929 data points for each mixing experiment. Control experiments were included in which either parental 32D cells (12.0 $\times$ $10^6$ cells/mL) or LE1.15 cells (12.2 $\times$ $10^6$ cells/mL) preincubated with a 50-fold excess of unlabeled mEGF were mixed 1:1 with F-EGF to final concentrations of either 2.0 or 10 nM. At each cell density and concentration, a total of 10 consecutive mixing experiments were performed, and the data from each mix at a particular cell density and F-EGF concentration were added together to yield the final experimental data set. Background counts were determined by mixing 100 $\mu$L of cells at each density with 100 $\mu$L SFB. Each experimental data set was corrected for background and the vertically ($I_{vv}$) and horizontally ($I_{vh}$) polarized emission intensities were transformed to anisotropy values using the formula

$$r = \frac{(I_{vv}G) - (I_{vh})}{(I_{vv}G) + (2I_{vh})} \quad (1)$$

where the subscripts refer to the polarization state of the excitation and emission light, respectively, and $G$ is a correction factor for the differences in the two emission channels. For $G$-factor determination, the excitation beam was rotated from vertical to horizontal polarization using a polarization rotator (Special Optics), and vertically ($I_{hv}$) and horizontally ($I_{hh}$) polarized emission intensities of free F-EGF (1−15 nM) were collected. $G$-factors were calculated using the formula

$$G = \frac{I_{hh}}{I_{hv}} \quad (2)$$

*Real-Time Dissociation of F-EGF from LE1.15 Cells by Unlabeled mEGF Chase.* The rate of F-EGF dissociation from LE1.15 cells in the presence of excess unlabeled mEGF was determined using the T-format steady-state fluorometer described above with the following modifications: the FC.15 fluorescence cuvette was replaced with a standard 1 cm $\times$ 1 cm cuvette holder (Oriel) which accommodated a 40 $\times$ 3 $\times$ 3 mm fluorescence cuvette (Oriel). As in association experiments, the temperature of all instruments and reagents was maintained at 20 °C. For chase dissociation measurements, cells were harvested and washed as described for association experiments and resuspended in SFB at a density of 16.0 $\times$ $10^6$ cells/mL. This suspension was mixed with F-EGF to yield a cell density of 11.5 $\times$ $10^6$ cells/mL and F-EGF concentrations of either 3.67 or 9.16 nM and then allowed to equilibrate at 20 °C for 7 min. Following equilibration, 180 $\mu$L of this suspension was transferred to the fluorescence cuvette. Above the cuvette, a Hamilton syringe containing 150 $\mu$L of either 440 nM mEGF in SFB or 1.1 $\mu$M mEGF in SFB was bolted into place. The syringe was bolted to avoid disturbing the cuvette during remixing. At the start of the experiments, the contents of the syringe were rapidly hand-mixed with the contents of the cuvette to yield a final cell density of 6.25 $\times$ $10^6$ cells/mL, final F-EGF concentrations of either 2.0 or 5.0 nM, and final unlabeled mEGF concentrations of either 200 or 500 nM. Data were acquired at 0.7 s intervals starting 10 s before mixing for a total of 95 min (8134 points), and the approximate dead time for hand mixing was less than 5 s. At approximately 4 min intervals during data collection, the solution was remixed

using the Hamilton syringe to prevent cell settling. At each F-EGF concentration, a total of 4 mixing experiments were performed, and the data from each mix were added together for the final experimental data set for that F-EGF concentration. Background measurements were made using cells to which no F-EGF was added prior to mixing with 1.1 $\mu$M unlabeled mEGF. All experimental data sets were corrected for background and the vertically and horizontally polarized emission intensities were transformed to anisotropy using eq 1.

*Real-Time Dissociation of F-EGF from LE1.15 Cells by Dilution.* The rate of F-EGF dissociation from LE1.15 cells by perturbation of equilibrium through dilution was determined using instrumentation described above for chase dissociation experiments with the following modification: the Hamilton syringe was removed and all mixing was performed by hand using a Rainin P20 pipetman (Gilson). For dilution dissociation experiments, cells were harvested and washed as described for association experiments and resuspended in SFB at a density of $1.25 \times 10^8$ cells/mL. This suspension was mixed 1:1 with 200 nM F-EGF to a F-EGF concentration of 100 nM and a cell density of $6.25 \times 10^7$ cells/mL and allowed to equilibrate at 20 °C for 7 min. To begin dilution dissociation experiments, 8, 4, or 2.67 $\mu$L of equilibrated cell suspension was hand mixed in the fluorescence cuvette with SFB to a total volume of 200 $\mu$L to give final dilutions of 25-, 50-, and 75-fold, respectively. As in previous experiments, the temperature of all instruments and reagents was maintained at 20 °C. Data were acquired at 100 ms intervals starting 15 s before mixing for a total of 13.15 min (7895 points), and the approximate dead time for hand mixing was less than 20 s. At each dilution, a total of 12−15 mixing experiments were performed, and the data from each mix were added together for the final experimental data set for that dilution. Background counts were determined by collecting data from cell suspensions to which no F-EGF was added prior to mixing with SFB in the cuvette. All experimental data sets were corrected for background, and the vertically and horizontally polarized emission intensities were transformed to anisotropy using eq 1.

*Data Analysis.* To facilitate visual inspection of anisotropy data, data for all experiments were smoothed using the SigmaPlot 5.0 software (SPSS Inc.) running average function with a window of 5 data points. The smoothed data sets were then analyzed by global analysis fitting of the data using a nonlinear least-squares method (*42*). Recovered rate constants were independent of the smoothing window. For global analysis of association data, an exponential function, a one receptor-class model, or a two independent receptor-class model was used in the fitting routine. The rate equation used for the one receptor-class model was

$$\frac{d[\text{F-EGF}_{\text{bound}}]}{dt} = k_{\text{on}}[\text{F-EGF}_{\text{free}}][\text{EGFR}] - k_{\text{off}}[\text{F-EGF}_{\text{bound}}] \quad (3)$$

The rate equation used for the two independent receptor-class model was

$$\frac{d[\text{F-EGF}_{\text{bound}}]}{dt} = [\text{F-EGF}_{\text{free}}](k_{\text{on1}}[\text{EGFR}_1] + k_{\text{on2}}[\text{EGFR}_2]) - (k_{\text{off1}}[\text{F-EGF}_{\text{bound1}}] + k_{\text{off2}}[\text{F-EGF}_{\text{bound2}}]) \quad (4)$$

For each model, the observed anisotropy was calculated from the concentrations of the individual species using the formula

$$r_{\text{measured}} = (r_{\text{free}}([\text{F-EGF}_{\text{free}}]/[\text{F-EGF}_{\text{total}}])) + (r_{\text{bound}}([\text{F-EGF}_{\text{bound}}]/[\text{F-EGF}_{\text{total}}])) \quad (5)$$

The value for $r_{\text{free}}$ was determined from control experiments to be $0.0957 \pm 0.0004$, and the value for $r_{\text{bound}}$ was determined to be ~0.180. The exact value for $r_{\text{bound}}$ was determined during nonlinear fitting. The differential rate equations for each model tested were solved using the method of finite difference in a subroutine incorporated into the global analysis kernal (Globals Unlimited). While the association data alone was fit to the different models, the combined association and dilution dissociation data surface was fit with only the two independent receptor-class model described above. Chase dissociation data sets were fit to an exponential function using a nonlinear least-squared method in the global analysis software.

*Model Comparison.* To compare the one and two receptor-class models, the fitting variances obtained for each model were normalized to the fitting variance obtained for the exponential function. The statistical significance of any difference between these two variance ratios was determined using the *F*-statistic criterion (*43*) with a confidence interval of 95%.

*Error Analysis.* Error analysis of all fitting parameters was performed using the exhaustive search method as previously described (*39*). Briefly, to obtain the asymmetric standard deviation associated with the fitting parameter, the *F*-statistic criterion was utilized to determine a statistically significant increase in $\chi^2$. The parameter values on either side of the fitting minimum associated with the significant $\chi^2$ values represent the standard deviation for that fitting parameter. All programs for nonlinear least-squares analysis were written in Fortran 77 using the Lahey Fortran compiler (F77L/EM32) running in the 32-bit protected mode and were run on an Intel Celeron-based microcomputer.

## RESULTS

*Preparation of Fluorescein-Labeled EGF.* To apply fluorescence spectroscopy to the measurement of EGF anisotropy as EGF interacts with its receptor, it was necessary to label EGF with a fluorescent moiety. We have described the synthesis and purification of murine EGF labeled uniformly at the amino terminus with fluorescein isothiocyanate (FITC), the motion of which is rigidly coupled to EGF (*39*). More recently we described the synthesis and purification of a mutant of murine EGF in which histidine 22 was changed to tyrosine (*28*), the corresponding residue in the human hormone. H22Y-mEGF retained full affinity in competition binding assays and biological activity in receptor autophosphorylation assays when compared to the wild-type hormone (data not shown). Further, introduction of this mutation avoided problems associated with reaction of the fluorescent

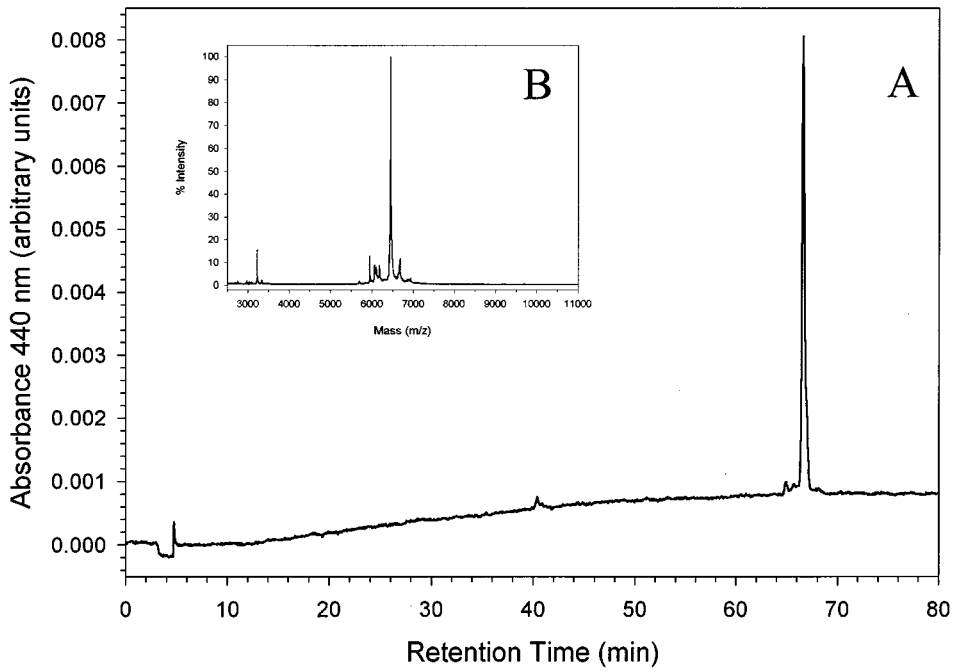


FIGURE 1: Characterization of F-EGF. Panel A is the $A_{440}$ chromatogram of the RP-HPLC experiment assessing the purity of the final F-EGF product. Panel B (inset) is the MALDI-TOF mass spectrum assessing the mass of the final F-EGF product. The $(m + 1)/z = 6456.21$ determined for the protonated F-EGF closely matched the calculated value of 6455.75.

probe with histidine 22, increasing the overall yield of the desired product. H22Y-mEGF was produced in *Escherchia coli*, purified to homogeneity, and reacted with FITC, and the resulting product (F-EGF) was purified by size-exclusion chromatography followed by RP-HPLC (Figure 1). Quantification of purified F-EGF was carried out as described (*39*), and mass spectrometry confirmed that each F-EGF molecule contained a single fluorescent moiety (Figure 1, inset). Since H22Y-mEGF contains only a single site at the amino terminus that is reactive with FITC, and our singly labeled product migrated as a single sharp peak by RP-HPLC, we concluded that F-EGF is labeled solely at the amino terminus.

*Cell Viability following Stopped-Flow Mixing.* To perform stopped-flow experiments using living cells, it was necessary to identify a suitable cell line capable of surviving the turbulent mixing process. Since ErbB receptors are capable of forming heterodimers upon ligand binding, it was also necessary to use a cell line that does not endogenously express any ErbB family protein, thus allowing control of the type and combination of receptors expressed. We chose the murine hematopoietic progenitor cell line 32D for our studies. Derived from continuous bone marrow cultures, 32D cells are undifferentiated cells that have been shown to be devoid of ErbB mRNAs and proteins (*44*, *45*) and, due to their hematopoietic lineage, seemed potentially more shear resistant to stopped-flow mixing than fibroblast or endothelial cells. 32D cells grow in suspension and do not form aggregates, simplifying experiments by eliminating the need to detach cells from substrate prior to experimentation and by preventing artifacts due to cell clumping. We tested the ability of 32D cells to withstand stopped-flow mixing using viability staining to detect dead cells. Exponentially growing cells were collected by centrifugation, washed free of residual medium, and resuspended in binding buffer at two times the desired final cell density for binding experiments. These cells were loaded into an SFM-4 stopped-flow unit and combined at a ratio of 1:1 with SFB at various flow rates, where the faster flow rates produce shorter dead times but greater shearing forces. Following mixing, cells were collected and stained with propidium iodide prior to assessing viability. When analyzed by flow cytometry, healthy cells show little propidium iodide staining (Figure 2A, top panel) relative to dead cells that readily take up the fluorescent dye (Figure 2A, bottom panel). From the flow cytometry histograms of stained cells mixed at each flow rate, we quantified the percentage of viable cells in each population. As seen in Figure 2B, there is very little change in 32D cell viability following turbulent mixing up to the maximum flow rate tested (4 mL/s).

While cell viability was not compromised at greater flow rates, we determined that when mixing difficult samples such as our cell suspensions, consistency of mixing improved when mixing was performed at slower flow rates (data not shown). Therefore, all subsequent stopped-flow mixing was performed at a flow rate of 0.67 mL/s, resulting in a calculated dead time of approximately 50 ms, acceptable for the purposes of this study.

*32D Cell Viability over Time.* Experiments designed to observe the kinetics of F-EGF interaction with EGF receptor-expressing 32D cells require that cells be maintained on ice over the course of several hours awaiting data collection. It was therefore necessary to determine how long cells remain viable when resuspended in binding buffer and stored on ice. 32D cells were harvested by centrifugation, washed free of residual medium, resuspended in stopped-flow buffer, and placed on ice. At 2 h intervals, aliquots of cells were removed and the percentage of viable cells in each sample was determined by flow cytometry as in Figure 2. Cell viability remained unchanged for up to 12 h while incubated on ice (data not shown). Additional experiments in which cells were subjected to turbulent mixing (0.67 mL/s flow rate) immediately prior to assessing viability at each time point

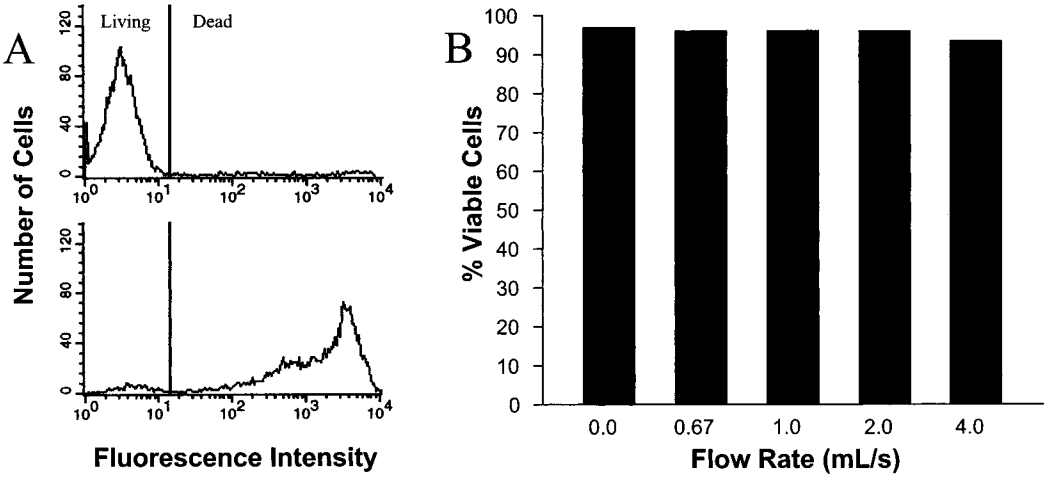


FIGURE 2: Viability of 32D cells following stopped-flow mixing. Panel A (top) is the flow cytometry histogram for a control sample of unmixed cells stained with propidium iodide. The indicated regions show cells considered to be either living or dead based on their fluorescence intensity. Panel A (bottom) is the flow cytometry histogram for a control sample of cells heat shocked for 30 min at 50 °C to induce cell death prior to staining. In panel B, 32D cells were subjected to stopped-flow mixing at flow rates up to 4.0 mL/s and then stained with propidium iodide. Flow cytometric analysis was performed as in panel A to determine the percentage of viable cells in each sample, and those values are plotted for each mixing speed. All subsequent stopped-flow mixing was performed at a flow rate of 0.67 mL/s.

showed no reduction in viability over time with the additional stress due to mixing (data not shown).

*Establishment of 32D Cells Expressing the EGF Receptor.* Since 32D cells do not express ErbB proteins, it was necessary to establish cells stably expressing the EGF receptor. We have previously described the establishment of a 32D subline (WT3) expressing the EGF receptor at approximately 100 000 receptors/cell (*28*). However, at this level of expression, it is necessary to prepare cell suspensions at very high densities (greater than $12 \times 10^6$ cells/mL) in order to obtain EGF receptor concentrations in the low nanomolar range for use in kinetic experiments. Because of the high turbidity of dense cell suspensions, spectroscopic measurements are difficult to make due to scattering artifacts introduced into the fluorescence data. We therefore sought to establish 32D-derived cell lines with levels of EGF receptor expression greater than that present in WT3 cells, allowing the use of lower cell densities while retaining EGF receptor concentrations in the low nanomolar range. We obtained the mammalian expression vector pLTR2-EGFR-neo (gift of P. P. Di Fiore) that has been shown to drive high levels of EGF receptor expression when used in 32D cells (*44*). This vector was transfected into 32D cells by electroporation, and resistant cells were selected through growth in antibiotic. Following selection, the uncharacterized population of cells was tested for EGF receptor expression by incubation with saturating levels of F-EGF prior to analysis by flow cytometry (data not shown). After confirmation of receptor expression, the population of transfected cells was incubated with F-EGF and then sorted to isolate clonal cell lines expressing the EGF receptor. Once putative clones grew to saturation, they were retested to determine relative EGF receptor expression and monoclonality. From this sorting protocol several monoclonal cell lines expressing the EGF receptor were obtained. One clonal 32D cell population in particular (named LE1.15) showed strong EGF receptor expression (Figure 3) and has been used for subsequent kinetic analysis. We estimate this cell line expresses approximately 5-fold more EGF receptors/cell than the WT3 subline (data not shown), allowing the use of much lower cell densities, and thus minimizing scattering artifacts due to cell turbidity. Retesting of cells after several weeks in culture showed no change in either EGF receptor expression levels or monoclonality (data not shown). Viability experiments performed on LE1.15 cells showed no change in the ability of cells to survive stopped-flow mixing (data not shown).

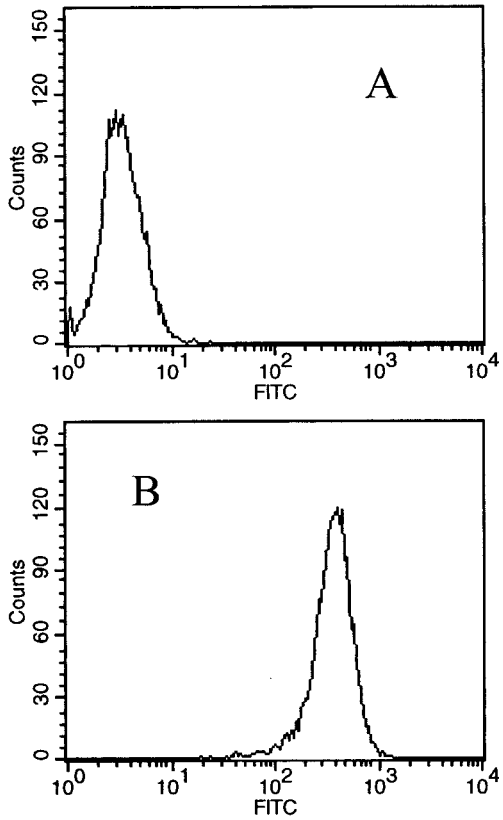


FIGURE 3: EGF receptor expression in LE1.15 cells. LE1.15 cells were incubated in the absence (panel A) or presence (panel B) of 20 nM F-EGF prior to analysis using flow cytometry. The increase in fluorescence intensity, as well as the shape of the histogram in panel B, is consistent with a monoclonal cell line expressing a high level of EGF receptor at the cell surface.

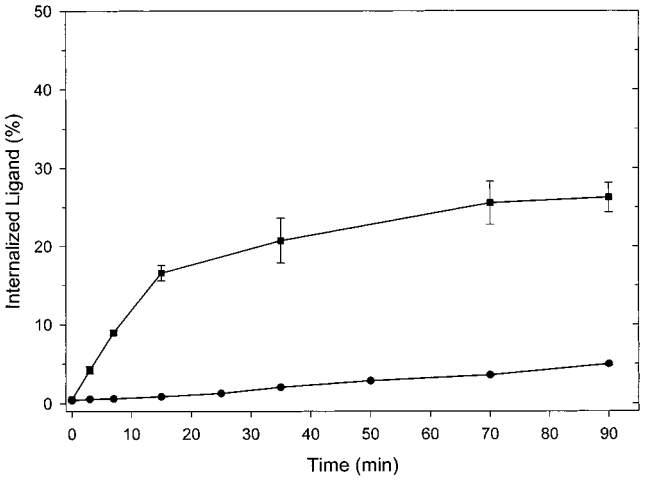


FIGURE 4: EGF receptor internalization in LE1.15 cells. LE1.15 cells ($10^6$ cells/sample) were incubated with $^{125}$I-rEGF (10 ng/mL) for 90 min at 4 °C. Following this incubation, cells were transferred to either 37 °C (squares) or 20 °C (circles) and incubated for the indicated time periods. Following incubation cells were immediately placed on ice. To remove free $^{125}$I-rEGF from cell associated $^{125}$I-rEGF, cells were sedimented through a cushion of fetal bovine serum. Cell pellets were washed twice with an acidic ligand-strip solution and then solublized. The proportion of cell-associated $^{125}$I-rEGF was determined by comparing the amount of radioactivity in the solublized cell pellets to the total cell-associated radioactivity (acid washes + cell pellets). Data presented represent the average ± the standard error of four determinations. Error bars for data at 20 °C are shown; however, the range is smaller than the size of the symbols used for each point. Compared to WT3 cells (which express lower levels of EGF receptor) the amount of EGF receptor internalization in LE1.15 cells at 37 °C is lower (maximum internalization for LE1.15 cells is 25% compared to 50% for WT3 cells; data not shown), consistent with saturation of the endocytic pathway due to higher levels of EGF receptor expression in LE1.15 cells.

*Internalization of EGF Receptor at 20 °C.* One concern about performing kinetic experiments using intact cells involves the possible internalization of receptor and bound ligand by way of the clathrin-mediated endocytosis pathway (*46*). This internalization of the EGF receptor upon ligand binding is temperature dependent: at 4 °C no internalization occurs, yet at 37 °C internalization is rapid (*47*). Since kinetic experiments may require data collection for more than 1 h, it was necessary to determine whether significant internalization occurs at the temperature used for these experiments. We found that internalization of the EGF receptor in LE1.15 cells is negligible (less than 1% internalized by 15 min and less than 5% internalized by 90 min when experiments were performed at 20 °C, Figure 4), suggesting that internalization has no significant effect on the measurement of EGF binding over the time scale required for completion of kinetic experiments.

*Real-Time Measurement of F-EGF Association to LE1.15 Cells.* To determine the kinetic rate constants for F-EGF binding to LE1.15 cells, the anisotropy of F-EGF was measured as a function of time at various concentrations of F-EGF and multiple densities of cells using the SFM-4 stopped-flow mixing unit coupled to a T-format steady-state fluorometer designed to monitor rapid anisotropy changes. Measurements of F-EGF binding to LE1.15 cells were carried out at each of three final densities ($6.1 \times 10^6$, $2.9 \times 10^6$, and $1.6 \times 10^6$ cells/mL) by mixing 1:1 with F-EGF stocks to yield final F-EGF concentrations of 1.0, 1.5, 2.0, 3.0, 5.0, 7.5, 10.0, and 15.0 nM. This range of F-EGF concentrations corresponds to levels both above and below the estimated EGF receptor concentration at each of the three cell densities (approximately 8, 4, and 2 nM, respectively). Control experiments consisted of either parental 32D cells mixed with 2.0 or 10.0 nM F-EGF (data not shown) or LE1.15 cells incubated with an excess of unlabeled mEGF prior to mixing with either 2.0 nM (Figure 5) or 10.0 nM (data not shown) F-EGF. The temperature of all instruments and reagents was maintained at 20 ± 1.0 °C. The resulting data surface (10 308 data points shown, 190 296 data points total, excluding preblocked controls) is shown in Figure 5.

Inspection of the data surface shows that for each curve, a monotonic increase in anisotropy over time is observed. The amplitude of each curve is consistent with changing experimental conditions: as the concentration of added F-EGF is increased at a given cell density, the amplitude of the curve decreases, consistent with the presence of more free F-EGF. Also, at a given concentration of added F-EGF, decreasing the cell density, and thus effective receptor concentration, reduces the amplitude of each binding curve. Finally, F-EGF binding is specific: no change in F-EGF anisotropy is observed in control experiments using either parental 32D cells (data not shown) or LE1.15 cells incubated with an excess of unlabeled mEGF prior to mixing (Figure 5).

*Measurement of F-EGF Dissociation from LE1.15 Cells by Excess mEGF Chase.* The association experiments described above allow for the determination of both association and dissociation rate constants. However, under the conditions described above, association dominates binding as the system approaches equilibrium, and therefore, the dissociation rate constants are not as well defined. To more accurately determine these dissociation constants for F-EGF bound to LE1.15 cells, we observed the dissociation of F-EGF from cells in the presence of a 100-fold excess of unlabeled mEGF. Cells were allowed to equilibrate with F-EGF, and then F-EGF anisotropy was measured as a function of time following mixing with a 100-fold excess of unlabeled mEGF (Figure 6). The final cell density was $6.0 \times 10^6$ cells/mL, and the final F-EGF concentrations were either 2.0 or 5.0 nM. Since data collection for this experiment extended to 95 min, and since 32D cells will begin to settle out of solution over this amount of time, it was necessary to use a different mixing protocol than described for association experiments. Rather than using the stopped-flow unit, the equilibrated F-EGF/cell suspension was placed in a $40 \times 3 \times 3$ mm fluorescence cuvette, and at time zero the solution of buffer containing the unlabeled mEGF was mixed using a Hamilton syringe bolted into place above the cuvette. At frequent intervals (approximately every 4−6 min) the suspension was remixed using the Hamilton syringe in order to keep cells in suspension. All other equipment, including excitation and emission optics as well as all electronics, was identical to that used in the association experiment.

*Measurement of F-EGF Dissociation from LE1.15 Cells by Perturbation of Equilibrium.* While methods employing an unlabeled "chase" component are commonly performed for the determination of dissociation rate constants, there are several limitations to this approach including (1) the potential for ligand-induced dissociation, (2) the perturbation of global

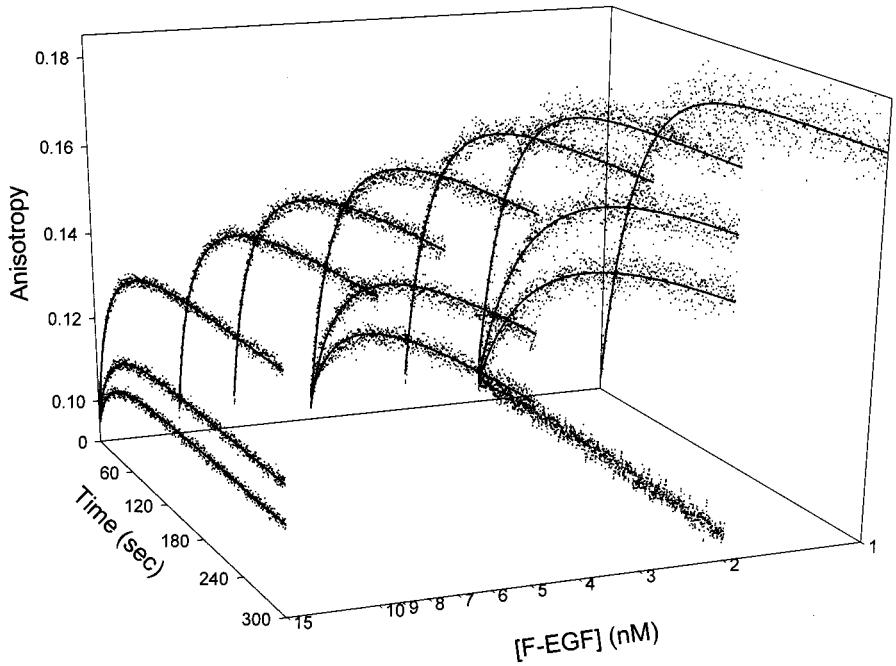


FIGURE 5: Real-time association of F-EGF to LE1.15 cells. LE1.15 cells at each of three final cell densities ($6.1 \times 10^6$, $2.9 \times 10^6$, and $1.6 \times 10^6$ cells/mL) were mixed with F-EGF to final concentrations of 1.0, 1.5, 2.0, 3.0, 5.0, 7.5, 10.0, and 15.0 nM for a total of 24 mixing experiments. This figure shows the anisotropy vs time for 13 of the 24 plots: shown are all mixing experiments performed at $6.1 \times 10^6$ cells/mL (excluding 1.5 nM F-EGF), as well as mixing experiments performed at 2.0, 5.0, and 15.0 nM F-EGF for both $2.9 \times 10^6$ and $1.5 \times 10^6$ cells/mL. At the 2.0 nM concentration, a representative control experiment is shown in which the EGF receptor sites ($6.1 \times 10^6$ cells/mL final density) were preblocked with a 50-fold excess of mEGF prior to mixing with F-EGF. Each mixing experiment yielded 7929 data points of which every 10th point is plotted. The fit lines represent the results of fitting a combined data surface (213 981 points total) including all 24 plots from this experiment, as well as the plots from the dilution dissociation experiment (Figure 7), to the two independent receptor-class model (eq 4). The parameter values recovered from this analysis are shown in Table 1.

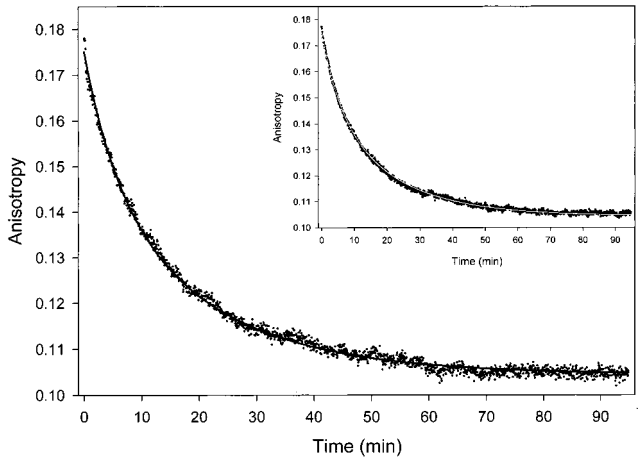


FIGURE 6: Chase dissociation of F-EGF from LE1.15 cells. LE1.15 cells were equilibrated with F-EGF prior to mixing with a 100-fold excess of unlabeled mEGF to give a final cell density of $6.25 \times 10^6$ cells/mL, final F-EGF concentrations of 2.0 nM or 5.0 nM (inset), and final mEGF concentrations of 200 nM or 500 nM (inset). This figure shows anisotropy vs time plots for each experiment and for each plot every 10th data point is shown. The fit lines in both plots represent the results from analysis using a two exponential decay function. This analysis recovered two dissociation rates of $0.29 \times 10^{-2}$ s$^{-1}$ (0.26, 0.33; SD) and $0.84 \times 10^{-3}$ s$^{-1}$ (0.78, 0.89; SD), and the normalized amplitudes of each process are $38 \pm 6\%$ and $62 \pm 6\%$, respectively.

receptor states due to receptor occupancy by unlabeled ligand, and (3) the large amount of chase reagent required. To circumvent these potential problems, we also measured dissociation rates by perturbation of equilibrium through dilution. LE1.15 cells were equilibrated with F-EGF under conditions in which the large majority of F-EGF was bound ($62.5 \times 10^6$ cells/mL, 100 nM F-EGF). Under these conditions, dilution of the system will cause a reequilibration resulting in the dissociation of F-EGF from the receptor. Following equilibration at 20 °C, cell/F-EGF suspensions were diluted 25-, 50-, and 75-fold and the resulting F-EGF dissociation was observed by monitoring changes in ligand anisotropy (Figure 7). As with "chase" dissociation experiments, hand mixing was performed but utilized a P20 pipetman rather than a Hamilton syringe. Since data collection for this experiment was taken out to 13 min, remixing of the samples was performed by hand pipetting approximately 6 min into data collection to keep cells in suspension. All optics and electronics were identical to those used in the association and the chase dissociation experiments. Observation of the resulting data surface shows a monotonic decrease in anisotropy for each curve, consistent with ligand dissociation as a result of reequilibration. The amplitude of each curve is consistent with the relative amount of dilution: greater dilution causes greater perturbation in equilibrium and, therefore, a larger change in anisotropy as the system reequilibrates.

*Global Analysis of Real-Time Data.* In the past, EGF binding to its receptor has generally been described by either a one receptor-class model or a two independent receptor-class model. To determine the model-dependent rate constants for F-EGF binding to LE1.15 cells, kinetic data (association, chase dissociation, and dilution dissociation) were subjected to global analysis using an empirical exponential function as well as one and two independent receptor-class kinetic models. The association data surface was initially fit using an exponential function, and at least two

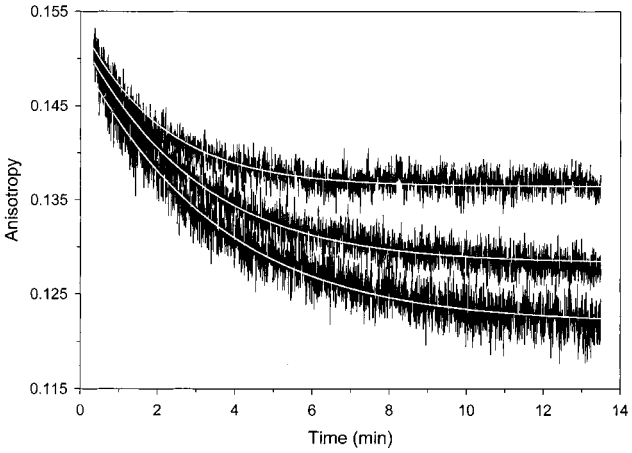


FIGURE 7: Dilution dissociation of F-EGF from LE1.15 cells. LE1.15 cells were equilibrated with F-EGF to give a final cell density of $6.25 \times 10^7$ cells/mL and a final F-EGF concentration of 100 nM. This suspension was then mixed by hand with SFB to give final dilutions of 25-fold (top curve), 50-fold (middle curve), and 75-fold (bottom curve). This figure shows anisotropy vs time plots for each dilution. For each plot, all data points (7895 total) are shown. To present clear separation of the data for the three dilution experiments, sequential data points are connected by a line, resulting in the different appearance of the data in this figure as compared with those of Figures 5 and 6. The fit lines represent the results of fitting a combined data surface (213 981 points total) including all 3 plots from this experiment, as well as the plots from the association experiment (Figure 5), to the two independent receptor-class model (eq 4). The parameter values recovered from this analysis are shown in Table 1.

exponential terms were required to describe the data surface. This analysis resulted in a fit with minimal variance, which was expected on the basis of the large number of fitting parameters and the minimal number of constraints imposed. To compare both the one and two independent receptor-class models, variances from each were normalized to the minimal fitting variance obtained from the exponential analysis. By this method, better fitting models would have variance ratios that approach 1.0. In fitting the association data surface, we obtained variance ratios of 1.16 for the one receptor-class model and 1.08 for the two independent receptor-class model. On the basis of confidence interval determination, these values represent a significant difference between these two models, with the two independent receptor-class model clearly providing the better statistical fit to the data surface. Once the two independent receptor-class model was determined to fit the association data well, the data surface was expanded to include dilution dissociation data. As with the association data surface alone, the combined association/dilution dissociation data surface was fit well by a two independent receptor-class model (fit curves in Figures 5 and 7) and the recovered kinetic parameters are reported in Table 1. Inclusion of dilution dissociation data in fitting had little effect on the recovered parameters relative to fitting association data alone (data not shown). The values reported in Table 1 are comparable to values determined in previous studies using A431 membrane vesicles as a source of EGF receptor (*39*).

Chase dissociation data were analyzed using an empirical exponential analysis in which it is assumed no rebinding of dissociated F-EGF occurs due to the presence of excess unlabeled mEGF. Nonlinear analysis of the chase dissociation data required two exponential terms to fit the data (fits

Table 1: Recovered Parameters from Global Analysis of Combined Association/Dilution Dissociation Data Using the Two Independent Receptor-Class Model

| parameter | fit value | − std dev[a] | + std dev |
|---|---|---|---|
| $k_{on1}$ | $8.6 \times 10^6$ M$^{-1}$ s$^{-1}$ | $5.60 \times 10^6$ | $12.7 \times 10^6$ |
| $k_{on2}$ | $2.4 \times 10^6$ M$^{-1}$ s$^{-1}$ | $2.01 \times 10^6$ | $2.54 \times 10^6$ |
| $k_{off1}$ | 0.0017 s$^{-1}$ | UD[b] | 0.0036 |
| $k_{off2}$ | 0.0021 s$^{-1}$ | 0.00164 | 0.00236 |
| [EGFR] low[c,g] | 2.6 nM | 2.51 | 2.64 |
| [EGFR] med[d,g] | 4.1 nM | 3.95 | 4.15 |
| [EGFR] high[e,g] | 8.6 nM | 8.3 | 8.8 |
| [EGFR] dil[f,g] | 68.4 nM | 65.5 | 71.5 |
| % $R_1$[h] | 12.6 | 7.5 | 33.0 |
| $R_{bound}$ | 0.181 | 0.179 | 0.183 |

[a] The standard deviation for all parameters was determined using 45 000 degrees of freedom for the analysis. The actual degrees of freedom for this calculation were 213 924, a number that was too large for our statistical software. Therefore, the standard deviations reported will be larger than they actually are. [b] Undetermined. [c] Concentration of receptor in $1.6 \times 10^6$ cells/mL suspension. [d] Concentration of receptor in $2.9 \times 10^6$ cells/mL suspension. [e] Concentration of receptor in $6.1 \times 10^6$ cells/mL suspension. [f] Concentration of receptor in dilution dissociation cell suspension. [g] Though the recovered concentrations of EGF receptors for each experiment generally agree with the cell densities used, some deviation is observed. We attribute this to difficulties in accurately determining cell density for each experiment, since cell suspensions must be diluted prior to determining density either by coulter counting or spectrophotometry. [h] Fraction of total receptors associated with $k_{on1}$ and $k_{off1}$, with the remaining fraction of receptors associated with $k_{on2}$ and $k_{off2}$.

overlaying the data points, Figure 6), and independent analysis of dissociation data at different concentrations of F-EGF failed to show any concentration dependence in either dissociation rates or amplitudes. The recovered rate constants for these dissociation processes are $0.29 \times 10^{-2}$ s$^{-1}$ (0.26, 0.33; SD) and $0.84 \times 10^{-3}$ s$^{-1}$ (0.78, 0.89; SD). These rate constants are in reasonable agreement with those recovered from the combined association/dilution dissociation data surface (0.0029 s$^{-1}$ vs 0.0021 s$^{-1}$; 0.00084 s$^{-1}$ vs 0.0017 s$^{-1}$) and support the presence of two distinct receptor classes at the surface of 32D cells. Furthermore, the similar results obtained in chase and dilution dissociation experiments, together with the lack of concentration dependence in the chase dissociation experiments, suggest that little, if any, ligand-induced dissociation occurs in the chase dissociation experiments, and recovered rate constants from these experiments accurately reflect intrinsic dissociation. The amplitudes of each chase dissociation rate, however, differ from those expected for these concentrations of F-EGF based on the recovered rate constants and receptor fractions from fitting the combined data surface. In the chase dissociation experiment, 38 ± 6% of the dissociating ligand was associated with the fast off-rate, with the remaining 62 ± 6% associated with the slow off-rate. By contrast, using the recovered parameters shown in Table 1 as well as the concentration of receptor and added F-EGF used in the chase dissociation experiment, the predicted percentages are 71% associated with the fast off-rate and 29% associated with the slow off-rate, values that are clearly different than those recovered from the chase dissociation experiment. While the nature of this difference is unclear, the most likely explanation is the presence of a large excess of unlabeled mEGF used in the chase dissociation experiments. In the association and dissociation experiments, receptor occupancy is changing throughout the observations, whereas in the chase dissocia-

tion experiments, receptor occupancy remains essentially constant throughout observation due to the excess unlabeled ligand present.

## DISCUSSION

To date several groups have characterized the kinetic interaction of EGF with its receptor, principally by measuring radioligand or fluorescent ligand binding to cultured cells or via SPR experiments using purified proteins. While all of these methods have been useful in advancing our understanding of EGF binding to the EGF receptor, each of these techniques has its limitations, and there has been little agreement among the reported rate constants measured by these varied techniques. Since the kinetics that govern the interactions between signaling molecules at the cell surface are critical in their functions, a method that combines the advantages of these methods would therefore be useful.

Stopped-flow mixing techniques have been applied to study the kinetics of many biological processes, including protein/protein and protein/DNA interactions (*48*, *49*), protein folding (*50*), and enzyme kinetics (*51*) among others. For the purposes of making kinetic measurements, particularly when examining macromolecular interactions, stopped-flow mixing has often been coupled with fluorescence detection methods. Fluorescence-based approaches allow for the examination of kinetic processes through measurements of fluorescence intensity changes, macromolecular anisotropy, or both. Previously, the majority of kinetic studies employing stopped-flow mixing and fluorescence detection have been limited to examining purified proteins or cell membrane preparations in vitro. The shear forces associated with turbulent stopped-flow mixing have restricted the use of intact cells due to the fragile nature of most cultured cell lines. One notable exception to this is a study by Nolan et al. (*52*), in which stopped-flow mixing was combined with flow cytometry for the observation of ligand/receptor interactions in living cells. In this study a Bio-logic SFM-3 mixing unit was modified to avoid turbulent mixing and to reduce flow rates, thus reducing shearing and meeting the flow rate requirements of the flow cytometer. Although this study demonstrated the applicability of stopped-flow mixing using intact cells with instrumental dead times on the order of 300 ms, no rigorous examination of ligand/receptor binding kinetics was reported, and no subsequent kinetic studies of which we are aware have employed these techniques for further examination of ligand/receptor interactions in intact cells.

This study extends the application of stopped-flow fluorescence anisotropy detection to the investigation of kinetic interactions between EGF and the EGF receptor expressed at the surface of intact cells. To ensure that changes in the motion of the probe truly reflect changes in the motion of the protein, a fluorescent derivative of murine EGF to which the probe is motionally coupled was synthesized and purified using established methods. Furthermore, all the F-EGF molecules were labeled at an identical single site, so that differences in binding properties as a result of ligand heterogeneity are avoided. While most mammalian cell lines cannot survive the shear forces associated with rapid stopped-flow mixing, we determined that the murine hematopoietic progenitor cell line, 32D, is capable of surviving rapid turbulent mixing with calculated dead times as short as 10 ms. Through stable transfection we have established monoclonal 32D cell lines expressing the EGF receptor in the absence of other ErbB family members for use in measuring hormone capture and release by living cells in real-time. Following rapid mixing, association of F-EGF to receptor-expressing 32D cells was observed by measuring changes in fluorescence anisotropy over time. Additionally, we used F-EGF anisotropy measurements to observe F-EGF dissociation from receptor-expressing cells. Dissociation was measured by two methods: first by chase dissociation of bound F-EGF in the presence of unlabeled mEGF; second by perturbation of equilibrium through dilution. All measurements were performed at various concentrations of F-EGF in the nanomolar range and various cell densities. To our knowledge this study represents the first real-time measurement of F-EGF capture and release by living cells expressing the EGF receptor in the absence of other ErbB family members.

Following rigorous global analysis of association data employing exponential as well as one receptor-class and two independent receptor-class kinetic models, we determined that a two independent receptor-class model best describes the data. While the nature of the two independent receptor classes suggested from the analysis remains unclear, it is clear that the two receptor classes cannot be explained by ErbB receptor heterodimerization (*28*), since the cells used in these experiments express the EGF receptor in the absence of other ErbB proteins. By analyzing the data surface including association and dilution dissociation data, we obtained association rate constants of $k_{on1} = 8.6 \times 10^6$ $M^{-1}$ $s^{-1}$ and $k_{on2} = 2.4 \times 10^6$ $M^{-1}$ $s^{-1}$ and dissociation rate constants of $k_{off1} = 0.17 \times 10^{-2}$ $s^{-1}$ and $k_{off2} = 0.21 \times 10^{-2}$ $s^{-1}$. Independent exponential analysis of chase dissociation data required two exponential terms to achieve the best fit ($k_{off1} = 0.84 \times 10^{-3}$ $s^{-1}$ and $k_{off2} = 0.29 \times 10^{-2}$ $s^{-1}$), further supporting the presence of two independent receptor-classes at the cell surface. Examination of the magnitudes of the recovered rate constants suggests that under physiological conditions, in which cells are transiently exposed to nanomolar concentrations of ligand, ligand capture *and* release occurs on a time scale (seconds to minutes) similar to that of many events in early receptor signaling, including dimerization, autophosphorylation, and internalization. Therefore the capture and release of ligand may function as the first line of physiological regulation of the EGF receptor-induced signal transduction cascade.

We have analyzed our data using the two independent receptor-class model due in large part to its prevalence in the literature and its success at fitting previous binding data. While the fits obtained using this model suggest it is adequate for describing the binding process, this model is unsatisfactory in the sense that it does not take into account known changes in the state of the EGF receptor, such as dimerization, phosphorylation, or association with cytoskeletal components. Moreover, we have reported experiments that further question the validity of using a two independent receptor-class model to describe the interaction of EGF with its receptor (*28*). Since the power of kinetic analysis lies more in refuting models than in proving that a given model is correct, it is necessary to consider that while the two independent receptor-class model provides the best statistical

fit to our data (the usual criterion for acceptance of a model), it may not be the best model to describe the interaction of EGF with the EGF receptor. We do not rule out the possibility that other kinetic models, such as those including dimerization or phosphorylation for example, may also describe our data. Though it is possible that current methods for observing EGF/EGF receptor binding may be insensitive to discrete steps of a more complex mechanism, in the context of intact cell experiments it may be possible to inhibit specific processes (such as dimerization) to functionally dissect each step of the binding process.

The EGF-like ligand family and the ErbB receptor family combine to form an intricate network of signaling molecules. Diversification of signaling within this network is complex and results from at least two sources: (1) the ability of a single EGF-like ligand to activate several potential combinations of ErbB heterodimers (*23*); (2) the ability of a single ErbB receptor to respond differently to individual EGF-like ligands (*53*). Recent work by Lenferink et al. (*29*) extends the idea that signal diversification within the ErbB network occurs not only as a result of receptor expression patterns but also as a result of different ligands activating the same receptor with different potencies. They show that despite similar affinities for the EGF receptor, members of a panel of EGF/TGFα chimeric proteins vary greatly in their potency for activating mitogen-activated protein kinase (MAPK) phosphorylation. Subsequent kinetic studies using in vitro SPR measurements showed that "superagonistic" chimeras, though displaying similar equilibrium binding constants compared to natural ligands, had enhanced association and dissociation rate constants for interaction with the expressed extracytoplasmic domain of the EGF receptor, suggesting that the dynamics of ligand/receptor exchange may play a more important role in determining signaling potency than equilibrium binding affinity. These differences in association and dissociation kinetics between different natural EGF-like ligands for the same ErbB receptor may in fact lead to different signaling outputs.

We have defined a system that may be used for the kinetic analysis of ligand binding to intact living cells. Since the parental cells used in these experiments do not express any endogenous ErbB protein, not only will it be possible to establish cells which coexpress any combination of ErbB receptors for use in determining the effects of heterodimerization upon the kinetics of ligand binding but it will also be possible to examine the kinetics of binding of several different EGF-like ligands to a single ErbB receptor or a particular combination of ErbB receptors. Further, this system allows the direct correlation of the kinetics of ligand−receptor interactions with intracellular signaling responses in the same population of intact living cells.

## ACKNOWLEDGMENT

We thank C. Leon for assistance in purifying F-EGF, Dr. Y. Zhen for mass spectrometric analysis, Dr. P. Di Fiore for providing the pLTR2-EGFR-neo expression vector, Dr. G. Carpenter for providing the 32D and WEH1-3B cells, Dr. W. Russell and M. Stevenson for providing $^{125}$I-rEGF, Dr. E. Hustedt for assistance in error analysis, Dr. C. Cobb for assistance in assembly of detection optics, and Dr. A. Beth for critical reading of the manuscript.

## REFERENCES

1. Wilkinson, J. C., Guyer, C. A., Beechem, J. M., and Staros, J. V. (1999) *Protein Sci. 8*, 150.
2. Wilkinson, J. C., Guyer, C. A., Staros, J. V., and Beechem, J. M. (2000) *Biophys. J. 78*, 69A.
3. Savage, C. R., Jr., Inagami, T., and Cohen, S. (1972) *J. Biol. Chem. 247*, 7612−21.
4. Carpenter, G., and Cohen, S. (1990) *J. Biol. Chem. 265*, 7709−12.
5. Derynck, R., Roberts, A. B., Winkler, M. E., Chen, E. Y., and Goeddel, D. V. (1984) *Cell 38*, 287−97.
6. Shoyab, M., McDonald, V. L., Bradley, J. G., and Todaro, G. J. (1988) *Proc. Natl. Acad. Sci. U.S.A. 85*, 6528−32.
7. Toyoda, H., Komurasaki, T., Uchida, D., Takayama, Y., Isobe, T., Okuyama, T., and Hanada, K. (1995) *J. Biol. Chem. 270*, 7495−500.
8. Shing, Y., Christofori, G., Hanahan, D., Ono, Y., Sasada, R., Igarashi, K., and Folkman, J. (1993) *Science 259*, 1604−7.
9. Higashiyama, S., Abraham, J. A., Miller, J., Fiddes, J. C., and Klagsbrun, M. (1991) *Science 251*, 936−9.
10. Holmes, W. E., Sliwkowski, M. X., Akita, R. W., Henzel, W. J., Lee, J., Park, J. W., Yansura, D., Abadi, N., Raab, H., Lewis, G. D., Shepard, H. M., Kuang, W. J., Wood, W. I., Goeddel, D. V., and Vandlen, R. L. (1992) *Science 256*, 1205−10.
11. Carraway, K. L., 3rd, Weber, J. L., Unger, M. J., Ledesma, J., Yu, N., Gassmann, M., and Lai, C. (1997) *Nature 387*, 512−6.
12. Zhang, D., Sliwkowski, M. X., Mark, M., Frantz, G., Akita, R., Sun, Y., Hillan, K., Crowley, C., Brush, J., and Godowski, P. J. (1997) *Proc. Natl. Acad. Sci. U.S.A. 94*, 9562−7.
13. Harari, D., Tzahar, E., Romano, J., Shelly, M., Pierce, J. H., Andrews, G. C., and Yarden, Y. (1999) *Oncogene 18*, 2681−9.
14. Riese, D. J., 2nd, and Stern, D. F. (1998) *Bioessays 20*, 41−8.
15. Ullrich, A., Coussens, L., Hayflick, J. S., Dull, T. J., Gray, A., Tam, A. W., Lee, J., Yarden, Y., Libermann, T. A., Schlessinger, J., Downward, J., Mayes, E. L. V., Whittle, N., Waterfield, M. D., and Seeburg, P. H. (1984) *Nature 309*, 418−25.
16. Stein, R. A., and Staros, J. V. (2000) *J. Mol. Evol. 50*, 397−412.
17. Coussens, L., Yang-Feng, T. L., Liao, Y. C., Chen, E., Gray, A., McGrath, J., Seeburg, P. H., Libermann, T. A., Schlessinger, J., Francke, U., Levinson, A., and Ullrich, A. (1985) *Science 230*, 1132−9.
18. Kraus, M. H., Issing, W., Miki, T., Popescu, N. C., and Aaronson, S. A. (1989) *Proc. Natl. Acad. Sci. U.S.A. 86*, 9193−7.
19. Plowman, G. D., Whitney, G. S., Neubauer, M. G., Green, J. M., McDonald, V. L., Todaro, G. J., and Shoyab, M. (1990) *Proc. Natl. Acad. Sci. U.S.A. 87*, 4905−9.
20. Plowman, G. D., Culouscou, J. M., Whitney, G. S., Green, J. M., Carlton, G. W., Foy, L., Neubauer, M. G., and Shoyab, M. (1993) *Proc. Natl. Acad. Sci. U.S.A. 90*, 1746−50.
21. Hackel, P. O., Zwick, E., Prenzel, N., and Ullrich, A. (1999) *Curr. Opin. Cell Biol. 11*, 184−9.
22. Yarden, Y., and Schlessinger, J. (1987) *Biochemistry 26*, 1443−51.
23. Alroy, I., and Yarden, Y. (1997) *FEBS Lett. 410*, 83−6.
24. Scatchard, G. (1949) *Ann. N.Y. Acad. Sci. 51*, 660−672.
25. Gill, G. N., Bertics, P. J., and Santon, J. B. (1987) *Mol. Cell Endocrinol. 51*, 169−86.
26. Schlessinger, J., Schreiber, A. B., Levi, A., Lax, I., Libermann, T., and Yarden, Y. (1983) *CRC Crit. Rev. Biochem. 14*, 93−111.
27. Carpenter, G. (1987) *Annu. Rev. Biochem. 56*, 881−914.
28. Stein, R. A., Wilkinson, J. C., Guyer, C. A., and Staros, J. V. (2001) *Biochemistry 40*, 6142−54.
29. Lenferink, A. E. G., van Zoelen, E. J. J., van Vugt, M. J. H., Grothe, S., van Rotterdam, W., van de Poll, M. L. M., and O'Connor-McCourt, M. D. (2000) *J. Biol. Chem. 275*, 26748−53.

30. Mayo, K. H., Nunez, M., Burke, C., Starbuck, C., Lauffenburger, D., and Savage, C. R., Jr. (1989) *J. Biol. Chem. 264*, 17838−44.
31. Bellot, F., Moolenaar, W., Kris, R., Mirakhur, B., Verlaan, I., Ullrich, A., Schlessinger, J., and Felder, S. (1990) *J. Cell Biol. 110*, 491−502.
32. Waters, C. M., Oberg, K. C., Carpenter, G., and Overholser, K. A. (1990) *Biochemistry 29*, 3563−9.
33. Berkers, J. A., van Bergen en Henegouwen, P. P., and Boonstra, J. (1992) *J. Recept. Res. 12*, 71−100.
34. Zhou, M., Felder, S., Rubinstein, M., Hurwitz, D. R., Ullrich, A., Lax, I., and Schlessinger, J. (1993) *Biochemistry 32*, 8193−8.
35. Domagala, T., Konstantopoulos, N., Smyth, F., Jorissen, R. N., Fabri, L., Geleick, D., Lax, I., Schlessinger, J., Sawyer, W., Howlett, G. J., Burgess, A. W., and Nice, E. C. (2000) *Growth Factors 18*, 11−29.
36. O'Shannessy, D. J., and Winzor, D. J. (1996) *Anal. Biochem. 236*, 275−83.
37. Carraway, K. L., 3rd, and Cerione, R. A. (1993) *Biochemistry 32*, 12039−45.
38. Chung, J. C., Sciaky, N., and Gross, D. J. (1997) *Biophys. J. 73*, 1089−102.
39. Rousseau, D. L., Jr., Staros, J. V., and Beechem, J. M. (1995) *Biochemistry 34*, 14508−18.
40. Savage, C. R., Jr., and Cohen, S. (1972) *J. Biol. Chem. 247*, 7609−11.
41. Pinkas-Kramarski, R., Soussan, L., Waterman, H., Levkowitz, G., Alroy, I., Klapper, L., Lavi, S., Seger, R., Ratzkin, B. J., Sela, M., and Yarden, Y. (1996) *Embo. J. 15*, 2452−67.
42. Beechem, J. M. (1992) *Methods Enzymol. 210*, 37−54.
43. Johnson, M. L., and Frasier, S. G. (1985) *Methods Enzymol. 117*, 301−342.
44. Pierce, J. H., Ruggiero, M., Fleming, T. P., Di Fiore, P. P., Greenberger, J. S., Varticovski, L., Schlessinger, J., Rovera, G., and Aaronson, S. A. (1988) *Science 239*, 628−31.
45. Wang, L. M., Kuo, A., Alimandi, M., Veri, M. C., Lee, C. C., Kapoor, V., Ellmore, N., Chen, X. H., and Pierce, J. H. (1998) *Proc. Natl. Acad. Sci. U.S.A. 95*, 6809−14.
46. Sorkin, A. (1998) *Front. Biosci. 3*, d729−d738.
47. Carpenter, G., and Cohen, S. (1976) *J. Cell Biol. 71*, 159−71.
48. Bai, Y., Perez, G. M., Beechem, J. M., and Weil, P. A. (1997) *Mol. Cell Biol. 17*, 3081−93.
49. Bertram, J. G., Bloom, L. B., Turner, J., O'Donnell, M., Beechem, J. M., and Goodman, M. F. (1998) *J. Biol. Chem. 273*, 24564−74.
50. Lillo, M. P., Szpikowska, B. K., Mas, M. T., Sutin, J. D., and Beechem, J. M. (1997) *Biochemistry 36*, 11273−81.
51. Gutierrez, A., Doehr, O., Paine, M., Wolf, C. R., Scrutton, N. S., and Roberts, G. C. (2000) *Biochemistry 39*, 15990−9.
52. Nolan, J. P., Posner, R. G., Martin, J. C., Habbersett, R., and Sklar, L. A. (1995) *Cytometry 21*, 223−9.
53. Sweeney, C., and Carraway, K. L., 3rd. (2000) *Oncogene 19*, 5568−73.

BI010705T